

# Multiple Andreev reflection and critical current across a topological transition in superconducting nanowire junctions

Pablo San-Jose<sup>1</sup>, Jorge Cayao<sup>1</sup>, Elsa Prada<sup>2</sup>, Ramón Aguado<sup>1</sup>

<sup>1</sup>*Instituto de Ciencia de Materiales de Madrid (ICMM-CSIC), Cantoblanco, 28049 Madrid, Spain*

<sup>2</sup>*Universidad Autónoma de Madrid, Cantoblanco, 28049 Madrid, Spain*

(Dated: May 6, 2022)

We study transport in biased Josephson junctions made of nanowires with strong spin-orbit coupling, as it transitions into a topological superconducting phase for increasing Zeeman field  $B$ . Despite the absence of a fractional steady-state ac Josephson current in the topological phase, the dissipative Multiple Andreev Reflection current  $I_{dc}$  at different junction transparencies is particularly revealing. It exhibits unique features related to topology, such as the gap inversion, the formation of Majorana bound states, and fermion-parity conservation. In contrast, and rather surprisingly, the critical current  $I_c$  does not vanish at the critical point where the superconducting gap vanishes, exhibiting a discontinuous  $\partial I_c/\partial B$  instead. These results demonstrate the feasibility to probe the formation of Majorana states without the need of phase sensitive or noise-related measurements.

Semiconducting nanowires with a strong spin-orbit coupling in the proximity of s-wave superconductors and in the presence of an external magnetic field are a promising platform to study Majorana physics. Theory predicts that above a critical Zeeman field  $B_c \equiv \sqrt{\mu^2 + \Delta^2}$ , defined in terms of the Fermi energy  $\mu$  and the induced s-wave pairing  $\Delta$  [1, 2], the wire undergoes a topological transition into a phase hosting zero energy Majorana bound states (MBS) at the ends of the wire. Recent experiments have reported conductance measurements that support the existence of such MBSs at normal-superconductor (NS) junctions in InSb [3, 4] and InAs [5] semiconducting nanowires. The main result of these experiments is an emergent zero-bias anomaly (ZBA) in differential conductance  $dI/dV$  measurements as an external Zeeman field  $B$  increases. In this context, the ZBA results from tunnelling into the MBS [6–8]. Although these experiments are partially consistent with the Majorana interpretation [9], other mechanisms that give rise to ZBAs, such as disorder [10–12] and Kondo physics [13], cannot be completely ruled out. Moreover, the expected superconducting gap inversion was not observed.

Stronger evidence could be provided by the direct observation of non-Abelian Majorana interference (braiding) [14], or by transport in phase-sensitive superconductor-normal-superconductor (SNS) junctions. The latter approach, which typically involves the measurement of an anomalous “fractional”  $4\pi$ -periodic ac Josephson effect [15–17] is in principle much less demanding than an interference experiment. Realistically, however, such fractional current may be difficult to detect, since dissipation is expected to destroy it in the steady state regime. Although it has been shown that the anomalous Josephson current survives in the dynamics, such as noise and transients [18–20], simpler experimental probes into MBS are extremely desirable [21].

Here we propose the multiple Andreev reflection (MAR) current in voltage-biased SNS junctions [22, 23],  $I_{dc}(V)$ , as an alternative, remarkably powerful, yet simple tool to study the topological transition of junctions made of semiconducting nanowires. This is made pos-

sible by the direct effect that gap inversion, MBS formation and fermion-parity conservation have on  $I_{dc}$  at various junction transparencies. For vanishing normal transparency  $T_N$ ,  $I_{dc}(V)$  traces the closing and reopening of the superconducting gap at  $B_c$ ,  $\Delta_{\text{eff}} \sim |B - B_c|$ . This gap inversion can be shown to be a true topological transition by tuning the junction to perfect transparency  $T_N = 1$ . The dissipative MAR current  $I_{dc}(V \rightarrow 0)$  in this limit shows parity conservation effects in the presence of MBS that are just as significant as a fractional ac Josephson effect would be, but do survive in the steady state limit. Moreover, the detailed dependence of MAR as a function of  $T_N$  has the fundamental advantage over transport spectroscopy in NS junctions in that it contains information about the peculiar dependence of MBS hybridization with superconductor phase difference  $\phi$  and  $T_N$ , despite not requiring any external control of  $\phi$ . Similarly, we show that another important phase-insensitive quantity, the critical current  $I_c$ , has an anomalous behaviour across the topological transition. Despite the expectation that it should vanish with the superconducting gap at  $B_c$ , we show that it remains finite due to a significant continuum contribution, revealing the gap inversion only as discontinuity in  $\partial I_c/\partial B$ .

*Nanowire spectroscopy.*—A single one-dimensional (1D) nanowire in the normal state is modelled in terms of its effective mass  $m^*$ , spin-orbit coupling  $\alpha_{\text{so}}$  and Fermi energy  $\mu$ , Zeeman splitting  $B = g\mu_B\mathcal{B}$ , where  $g$  is the semiconductor’s  $g$ -factor and  $\mathcal{B}$  is the magnetic field along the wire. The wire is close to depletion, so  $\mu$  is not very large. Its normal Hamiltonian reads ( $\sigma_i$  are spin Pauli matrices)

$$H_0 = \frac{p^2}{2m^*} - \mu + B\sigma_x + \alpha_{\text{so}}\sigma_y p.$$

In the presence of an induced s-wave superconducting pairing  $\Delta$  (assumed real), the system is modeled by the Nambu Hamiltonian

$$H = \begin{bmatrix} H_0 & -i\Delta\sigma_y \\ i\Delta\sigma_y & -H_0^* \end{bmatrix}. \quad (1)$$

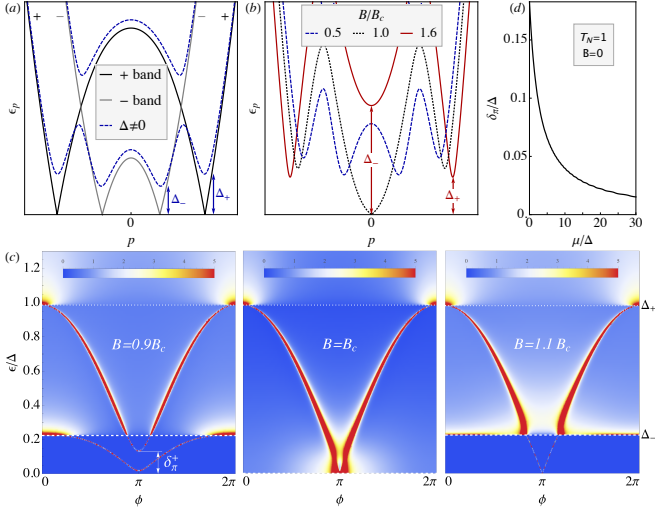


FIG. 1. (Color online) (a) Lowest bands of a  $B = 0.5B_c$  nanowire, with (dashed) and without (solid) pairing  $\Delta$ . (b) Evolution of bands with Zeeman field  $B$ . The gap  $\Delta_-$  closes at  $B = B_c$ , while  $\Delta_+$  does not. (c) Local density of states at the junction for perfect normal transparency  $T_N = 1$ , which is peaked at the energy  $\epsilon_\pm(\phi)$  of Andreev (quasi)bound states. The minimum  $\delta_\pm^\pm$  of  $\epsilon_\pm(\phi)$  for  $B < B_c$  falls to zero at perfect transparency as  $\mu/\Delta$  is increased (Andreev approximation). Panel (d) shows the  $T_N = 1$ ,  $B = 0$   $\delta_\pi^+ = \delta_\pi^-$ . It falls as  $\delta_\pi = c_1 \Delta^2 / (\mu + \Delta c_2)$  for some  $c_{1,2} > 0$ .

The essential ingredient for a topological superconductor is an effective p-wave pairing acting on a single (“spinless”) fermionic species, the so-called Kitaev model [15]. Spin-orbit coupling splits nanowire states into two subbands of opposite helicity at  $B = 0$ . At finite  $B$ , these two subbands, which we label + and − [black and gray lines in Fig. 1(a)], have spins canted away from the spin-orbit axis. The s-wave pairing  $\Delta$ , expressed in the  $\pm$  basis, takes the form of an intraband p-wave  $\Delta_p^{++/-/-}(p) = \pm i p \Delta \alpha_{\text{so}} / \sqrt{B^2 + (\alpha_{\text{so}p})^2}$ , plus an interband s-wave pairing  $\Delta_s^{+-}(p) = \Delta B / \sqrt{B^2 + (\alpha_{\text{so}p})^2}$  [24]. Without the latter, the problem decouples into two independent p-wave superconductors, while  $\Delta_s^{+-}$  acts as a weak coupling between them. Each quasi-independent sector has a different gap. These two ( $B$ -dependent) gaps, which we call  $\Delta_-$  (at small momentum) and  $\Delta_+$  (large momentum), are shown in Fig. 1(a,b). While  $\Delta_+$  remains roughly constant with  $B$  (for strong spin-orbit coupling),  $\Delta_-$  vanishes linearly as  $B$  approaches the critical field,  $\Delta_- \approx |B - B_c|$  [25]. This closing and reopening (gap inversion) signals a topological transition, induced by the effective removal of the − sector away from the low-energy problem. Below  $B_c$  the nanowire is composed of two (weakly coupled) spinless p-wave superconducting species, and is therefore topologically trivial. Above  $B_c$ ,  $\Delta_-$  is no longer a p-wave gap, but rather a normal (Zeeman) spectral gap already present in the normal state, transforming the wire into single-species p-wave superconductor with non-trivial topology. This phase is host

to pairs of MBSs at the wire ends, which are protected by the effective gap  $\Delta_{\text{eff}} = \text{Min}(\Delta_+, \Delta_-)$ . The same physics also emerges in the problem of superconducting helical edge states in spin-Hall insulators, which is spinless to start with [17, 18].

In a short Josephson junction made of two nanowires across a contact with normal transparency  $T_N$ , an Andreev bound state (ABS) is formed in each of the two sectors above for  $B < B_c$ , while only one, associated to  $\Delta_+$  is formed for  $B > B_c$ . Their energies  $\epsilon_\pm$  depend on the superconducting phase difference  $\phi$  across the junction, as shown in Fig. 1(c) (case  $T_N = 1$ ). Due to the residual  $\Delta_s$  coupling between the two sectors, the  $\Delta_+$  Andreev state is actually *quasibound* in the energy window  $\Delta_- < \epsilon < \Delta_+$ . Moreover, in the non-topological phase (left panel) their energy does not reach zero at  $\phi = \pi$ , unlike predicted by the standard theory for  $T_N = 1$  within the Andreev approximation  $\mu \gg \Delta$  [26]. The energy minimum  $\delta_\pi$  does indeed vanish as  $\mu/\Delta$  grows, see Fig. 1(d). In the topological phase (right panel), the surviving ABS associated to  $\Delta_+$  arises as the hybridisation of two MBS across the junction. Global fermion-parity conservation protects the  $\phi = \pi$  level crossing, giving exactly  $\delta_\pi = 0$ .

*ac Josephson in nanowire junctions.*—Here we are concerned with the effects of the topological transition in the transport across a short junction of two semi-infinite wires. We wish to compute, for different normal transparencies  $T_N$ , the MAR current  $I_{dc}(V)$  as a function of bias  $V$  across the junction, and the critical current  $I_c$  supported at  $V = 0$ . For computation purposes, we consider a discretisation of the continuum model Eq. (1) for each wire into a tight-binding 1D lattice with a small lattice spacing  $a$  [used also to compute Fig. 1(c,d)]. This transforms terms containing the momentum operator  $p$  into nearest-neighbour hopping matrices  $v$ . Namely  $H_0 = \sum_i c_i^+ h c_i + \sum_{\langle ij \rangle} c_j^+ v c_i + \text{h.c.}$ , where  $t = \hbar^2 / 2m^* a^2$  and the spin structure of  $h$  and  $v$  is

$$h = \begin{pmatrix} 2t - \mu & B \\ B & 2t - \mu \end{pmatrix}, \quad v = \begin{pmatrix} -t & \frac{\hbar}{2a} \alpha_{\text{so}} \\ -\frac{\hbar}{2a} \alpha_{\text{so}} & -t \end{pmatrix}.$$

The coupling across the junction is modelled by a hopping matrix  $v_0 = \nu v$  between the end sites of each wire, labeled  $l$  and  $r$ , that is suppressed by a dimensionless factor  $\nu \in [0, 1]$ , which controls the junction’s normal transparency at  $B = 0$ ,  $T_N(\nu)$ .

Under a constant voltage bias  $V$ , the pairings  $\Delta$  to the left and right of the junction acquire an opposite and time-dependent phase difference,  $\phi(t) = 2eVt/\hbar$ . This induces Landau-Zener transitions between the ABS and into the continuum, thereby developing a time dependent Josephson current with both  $I_{dc}$  and  $I_{ac}$  components. Such is the point of view exploited e.g. in Refs. [19 and 27]. Alternatively, the time dependence of  $\phi(t)$  can be gauged away into the hopping term across the junction, which then becomes  $v_0(t) = \nu e^{-i\omega_0 t \tau_z} \sum_{\sigma\sigma'} c_{r\sigma}^+ v_{\sigma\sigma'} c_{l\sigma'} + \text{h.c.}$ , where  $\tau_z$  is the  $z$ -Pauli matrix in Nambu space. Driving frequency is  $\omega_0 = eV/\hbar$ . By employing Keldysh-Floquet theory [28, 29], see Ap-

pendix, we obtain the stationary-state time-dependent current which contains all the harmonics of the ac Josephson effect, i.e.  $I(t) = \sum_n e^{in\omega_0 t} I_n$ . Here, we concentrate on the dc-current  $I_{dc} = I_0$  as a function of  $V$  and  $T_N$ . The results for  $I_{dc}(V)$  at small, intermediate and full transparency are summarised in Fig. 2(a-c) for increasing values of  $B$  spanning the topological transition (blue is the non-topological phase, red the topological one hosting MBS).

*Tunneling regime.*—As the junction's normal transparency  $T_N$  approaches zero in the non-topological regime, dc-transport vanishes below an abrupt thresholds voltage  $V_t = 2\Delta_{\text{eff}}/e = 2\Delta_-/e$  (Fig. 2(a), blue curves), where, recall,  $\Delta_{\text{eff}} = \text{Min}(\Delta_-, \Delta_+)$ . This well known result follows from the fact that there are no quasiparticle excitations in the decoupled wires for energy  $\epsilon \in (-\Delta_{\text{eff}}, \Delta_{\text{eff}})$  if  $B < B_c$ . Indeed, to second order in perturbation theory in  $\nu$ , the MAR current takes the form of a convolution between  $A_0(\omega)$  and  $A_0(\omega \pm eV/\hbar)$ , where  $A_0$  is the decoupled ( $\nu = 0$ ) spectral density at each side of the junction. [The trace of  $A_0(\epsilon)$ , proportional to the local density of states (LDOS), is shown in Fig. 3(a)]. Hence, as  $B$  increases, the tunnelling current threshold follows the closing of the gap in the LDOS, until  $V_t$  vanishes and  $I_{dc}$  becomes linear in small  $V$  at  $B_c$  (black curve). As  $B > B_c$ , the gap reopens, but the threshold is now halved to  $V_t = \Delta_{\text{eff}}/e$  (red curves) [30]. The change, easily detectable as a halving of the slope of the threshold  $dV_t/dB$  across  $B_c$ , is due to the emergence of an intra-gap zero-energy MBS in the topological phase [see zero energy peak in Fig. 3(a)], which opens a tunnelling transport channel from or into the new zero energy state. Moreover, as  $B$  is increased above a certain field  $B_c^{(2)}$ ,  $\Delta_-$  surpasses  $\Delta_+$ , and  $\Delta_{\text{eff}}$  saturates at  $\Delta_+$ . This is directly visible in  $V_t(B)$  as a kink at  $B_c^{(2)}$  [see dashed and dotted lines in Fig. 2(a)]. [31].

*Intermediate transparency regime.*—In higher transparency non-topological junctions, subharmonic MAR steps develop at voltages  $V_t/n = 2\Delta_{\text{eff}}/en$  ( $n = 2, 3, 4, \dots$ ), see Fig. 2(b). The specific profile of each step with  $V$  still contains information on the LDOS of the junction at energies around  $\Delta_{\text{eff}}$ . At  $B = 0$ , the power-law LDOS for  $|\epsilon| > \Delta$  results in a staircase-like curve  $I_{dc}(V)$  [blue line in Fig. 2(d)]. This shape is roughly preserved up to  $B = B_c$ . For  $B > B_c$  the MAR subharmonic profile changes qualitatively, however. The subharmonic threshold voltages  $V_t/n$  are halved (since  $V_t$  is halved), and the MAR current profile becomes oscillatory instead of step-like. A blowup of the oscillations is presented in Fig. 2(d) (red curve), together with guidelines for the corresponding  $V_t/n$  in gray.

The emergence of oscillatory MAR steps is connected to the formation of the zero energy MBS, specifically to the sharp zero energy peak in the LDOS that is a consequence of the localized nature of the MBS. This effect is well known from the studies of the MAR current in Josephson junctions containing a resonant level [32–34], such as for instance a quantum dot between two super-

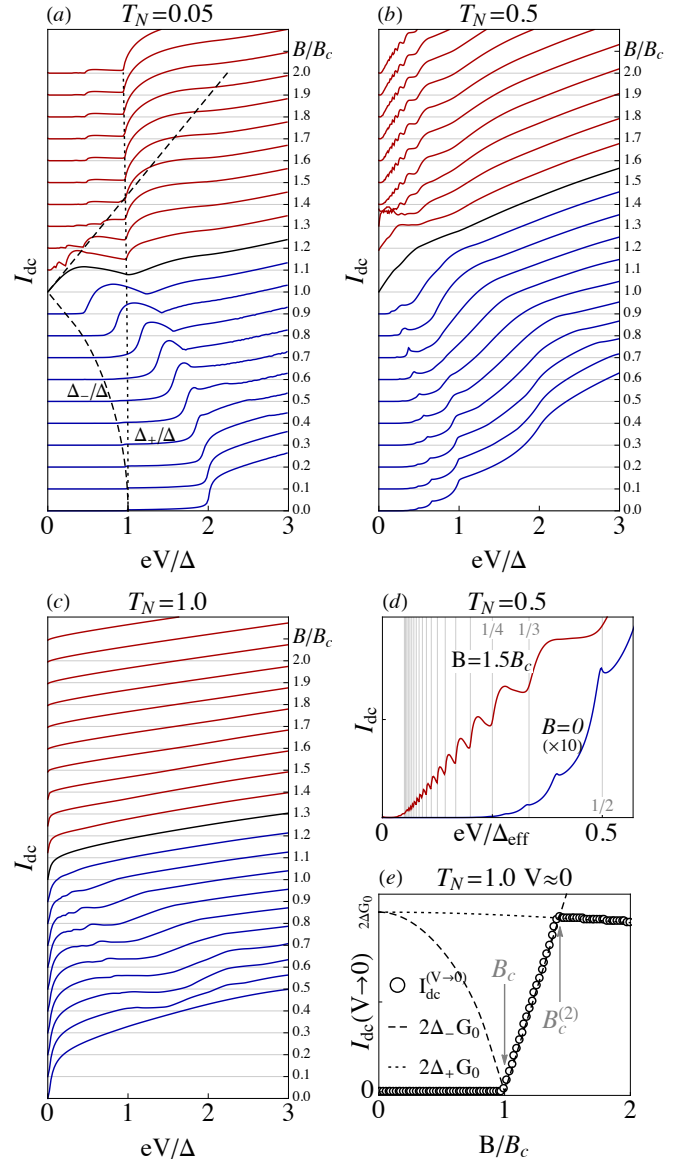


FIG. 2. (Color online) Time-averaged Josephson current  $I_{dc}$  as a function of bias  $V$  for increasing Zeeman field  $B$ . Curves are offset by a constant  $2\Delta_{\text{G}_0}/e$ , with  $\mathcal{G}_0 = e^2/\hbar$ . Blue and red curves correspond to the non-topological ( $B < B_c$ ) and topological ( $B > B_c$ ) phases respectively. Panels (a) to (c) show the cases of tunnelling, intermediate and full transparency. Panel (d) is a blowup of the low bias MAR subharmonics at intermediate transparency. Panel (e) shows the asymptotic  $I_{dc}(V \rightarrow 0)$  at full transparency (circles), along with the dependence of the quantities  $2\Delta_{-}\mathcal{G}_0$  and  $2\Delta_{+}\mathcal{G}_0$  with  $B$  across the topological transition [dashed/dotted lines, evolution also shown in panel (a)].

conductors. In the latter case, however, the oscillatory MAR subharmonics arise at odd fractions of  $2\Delta_{\text{eff}}$ , i.e. at voltages  $2\Delta_{\text{eff}}/(2n+1)e$ , instead of the  $\Delta_{\text{eff}}/en$  of the Majorana case. This difference is ultimately due to the fact that a quantum dot resonant level spatially localised within the junction cannot carry current directly into the

reservoirs of the external circuit, while a zero energy MBS (essentially half a non local fermion) can. This same situation arises in  $d$ -wave Josephson junctions [35], which also exhibit oscillatory  $\Delta_{\text{eff}}/eV$  MAR subharmonics owing to the presence of mid gap states.

*Transparent limit.*—In the limit  $T_N \rightarrow 1$ , ABS energies  $\epsilon_{\pm}(\phi)$  [Fig. 1(c)] touch the continuum at  $\phi = 0$ . From the Landau-Zener point of view of the ac Josephson effect [27], the time dependence of  $\phi(t) = 2eVt/\hbar$  for an arbitrarily small  $V$  will induce the escape of any quasiparticle occupying an ABS into the continuum after a single  $\phi(t)$  cycle. A given ABS becomes occupied with high probability in each cycle around  $\phi = \pi$  if the rate  $\hbar d\phi(t)/dt = 2eV$  exceeds its energy minimum  $\epsilon(\pi) \equiv \delta_{\pi}$ . At voltages exceeding such minimum, one quasiparticle is injected into the continuum per cycle, and a finite  $I_{dc}(V \gtrsim \delta_{\pi}/e)$  arises. Below such voltage, however, the ABS remains empty, so that if  $\delta_{\pi}^{\pm}$  is finite, as is the case of a realistic non-topological junction (see Fig. 1(c)), one obtains  $I_{dc}(V \rightarrow 0) = 0$  (valid for any transparency at  $B < B_c$ ). This is in contrast to the conventional  $B = 0$ ,  $T_N = 1$  result  $I(V \rightarrow 0) = 4\Delta\mathcal{G}_0/e$ , predicted within the Andreev approximation ( $\mathcal{G}_0 = e^2/h$ ).

After the topological transition this picture changes dramatically. The two MBS at each side of the junction hybridise for a given  $\phi$  into a *single* ABS. This seemingly innocent change has a notable consequence. Since fermion parity in the superconducting wires is globally preserved, an anticrossing at  $\phi = \pi$ , which would represent a mixing of a state with one and zero fermions in the lone ABS, is forbidden. Parity conservation therefore imposes  $\delta_{\pi} = 0$  in the presence of MBS, irrespective of  $T_N$  or  $\mu/\Delta$  [36]. This is a true topologically protected property of the junction, and gives rise to a finite  $I_{dc}(V \rightarrow 0) = 2\Delta_{\text{eff}}\mathcal{G}_0$ , i.e. half the value expected for the non-topological junction in the Andreev approximation. This abrupt change is shown in Fig. 2(c,e). The  $I_{dc}(V \rightarrow 0)$  MAR current in the transparent junction limit, therefore, directly probes the emergence of parity protected ABS crossings, formed by the fusion of the two Majorana modes in the junction.

*Critical current.*—For finite impedance of the external circuit, a  $V = 0$  supercurrent peak should arise superimposed onto the computed  $I_{dc}$  [22, 23, 37]. In the transparent limit, this peak may hinder the experimental identification of the  $I_{dc}(V \rightarrow 0)$  limit, but itself holds valuable information about the transition. The critical current  $I_c$  may be computed in general by maximizing the  $V = 0$  (time-independent) current  $I(\phi)$  respect to  $\phi$  (including the contribution from the continuum). For a short transparent junction at  $B = 0$ ,  $I_c$  is maximum, and equal to  $I_c^0 \equiv 4e\Delta/\hbar$ . Fig. 3(b) shows  $I_c$  for increasing values of the Zeeman field. Note that, in spite of the naive expectation that a nanowire without a superconducting gap should not carry a finite supercurrent, this is not the case. At  $B = B_c$ ,  $I_c$  is finite, while  $\Delta_{\text{eff}} = 0$  [the junction LDOS at criticality is also gapless, see Fig. 3(a)]. This gapless supercurrent comes from the  $\epsilon_{+}(\phi)$

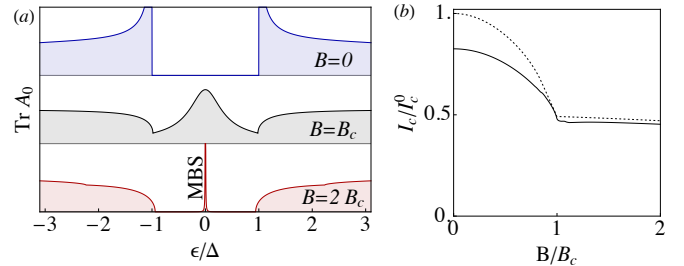


FIG. 3. (Color online) (a) Local density of states at the end of a single nanowire in the non-topological (top), critical (middle) and topological phase (bottom). A zero-energy Majorana peak appears in the latter case. (b) The critical current  $I_c(B)$  across the topological transition in units of  $I_c^0 = 4e\Delta/\hbar$ . The dotted line corresponds to  $\frac{1}{2}(\Delta_+ + \Delta_-)/\Delta$  for  $B < B_c$ , and  $\frac{1}{2}\Delta_+/\Delta$  for  $B > B_c$ .

quasi-bound Andreev state in the continuum, which contributes to the current almost as if it were a subgap ABS. It is thus a reasonable approximation to write  $I_c$  as the sum of the critical current from each ABS. For  $B < B_c$ ,  $I_c \approx \frac{1}{2}I_c^0(\Delta_+ + \Delta_-)/\Delta$ . The  $\Delta_-$  contribution, however, should not be included for  $B > B_c$ , leading to a discontinuous derivative  $\partial I_c/\partial B$  at  $B_c$  as a signature of the topological transition. This simple model gives a qualitative fit to the exact numerical results [dotted line in Fig. 3(b)], with deviations coming from corrections to the Andreev approximation, and contributions above  $\Delta_+$ .

In conclusion, we have shown that the steady state dc-current in biased Josephson junctions is a flexible experimental probe into the various aspects of the topological superconducting transition in semiconducting nanowires. Tuning the junction transparency one may obtain evidence of MBS formation as conclusive as a fractional Josephson effect, without requiring control of the junction phase. Moreover we have found that the critical current in the wire does not vanish at the transition due to above-gap contributions, although its derivative with  $B$  exhibits a discontinuity as a result of the disappearance of one Andreev bound state.

## ACKNOWLEDGMENTS

We acknowledge the support of the European Research Council, the Spanish Research Council CSIC through the JAE-Predoc Program (J. C.) and the Spanish Ministry of Economy and Innovation through Grants No. FIS2011-23713 (P.S.-J), FIS2009-08744 (E.P. and R.A.) and the Ramón y Cajal Program (E. P.).

## Appendix: Keldysh-Floquet theory

We present a summary of the Keldysh-Floquet theory employed in the computation of steady-state, time-averaged Josephson current  $I_{dc}$  through a biased

superconducting-insulating-superconducting junction, as a function of bias  $V$  and junction transparency.

Consider a mesoscopic system composed of two semi-infinite leads (labeled  $L$  and  $R$ ), each in thermal equilibrium at the same temperature  $T$  and with the same chemical potential  $\mu = 0$ . Each lead has a finite s-wave superconducting pairing  $\Delta_\alpha$ , where  $\alpha = L, R$ . A central system ( $\alpha = S$ ), which may or may not be superconducting, is coupled to both leads through operator  $v$ . In its Nambu form, the Hamiltonian of the system reads

$$\hat{H} = \frac{1}{2} \sum_{ij} (c_j | c_j^+ ) H_{ij} \left( \frac{c_j}{c_j^+} \right)$$

where the Nambu Hamiltonian matrix takes the general form

$$H = \left( \begin{array}{ccc|ccc} h_L & v^+ & 0 & \Delta_L & 0 & 0 \\ v & h_S & v^+ & 0 & \Delta_S & 0 \\ 0 & v & h_R & 0 & 0 & \Delta_R \\ \hline \Delta_L^+ & 0 & 0 & -h_L^* & (-v^+)^* & 0 \\ 0 & \Delta_S^+ & 0 & -v^* & -h_S^* & (-v^+)^* \\ 0 & 0 & \Delta_R^+ & 0 & -v^* & -h_R^* \end{array} \right)$$

Here  $h_\alpha$  is the normal Hamiltonian for each section of the system. The blocks delimited by lines denote the Nambu particle, hole and pairing sectors.

If we apply a left-right voltage bias  $V$  through the junction, the BCS pairing of the leads will become time dependent,  $\Delta_{L/R} \rightarrow e^{\pm iVt} \Delta_{L/R}$ , while  $h_{L/R} \rightarrow h_{L/R} \pm V/2$  (we take  $e = \hbar = 1$ ). Both these changes can be gauged away from the leads and into the system by properly redefining  $c_i^+ \rightarrow c_i^+(t) = e^{\pm iVt/2} c_i^+$ . This transformation is done also inside the system  $S$ , thereby effectively dividing it into two, the portion with an  $e^{iVt/2}$  phase (denoted  $S_L$ ), and the portion with the opposite phase (denoted  $S_R$ ). This restores  $H$  to its unbiased form, save for a new time dependence in  $h_S \rightarrow h_S(Vt)$ , which is constrained to the coupling between the  $S_L$  and  $S_R$ ,

$$h_S(Vt) = \begin{pmatrix} h_{S_L} & e^{-iVt} v_0^+ \\ e^{iVt} v_0 & h_{S_R} \end{pmatrix}$$

It is important to note that  $H(t)$  is periodic, with angular frequency  $\omega_0 = V$ . In the steady state limit (at long times  $t$  after switching on the potential  $V$ ) all response functions and observables will exhibit the same time periodicity (all transient effects are assumed to be completely damped away). In particular, the steady state current  $I(t) = I(t + 2\pi/\omega_0)$ , so that

$$I(t) = \sum_n e^{in\omega_0 t} I_n$$

for some harmonic amplitudes  $I_n$ , in general complex, that satisfy  $I_n = I_{-n}^*$  since  $I(t)$  is real.

This current can be computed using the Keldysh Green's function formalism. [38] The standard expression for  $I(t)$  is computed starting from the definition of

$I(t) = \partial_t N_L$ , where  $N$  is the total number of fermions in the left lead. By using Heisenberg equation and the Keldysh-Dyson equation, one arrives at

$$I(t) = \text{Re}[J(t)]$$

where

$$J(t) = \frac{2e}{\hbar} \int dt' \text{Tr} \{ [G^r(t, t') \Sigma_L^<(t', t) + G^<(t, t') \Sigma_L^a(t', t)] \tau_z \}$$

The z-Pauli matrix  $\tau_z$  above acts on the Nambu particle-hole sector,

$$\tau_z = \begin{pmatrix} \mathbb{1} & 0 \\ 0 & -\mathbb{1} \end{pmatrix}.$$

The self energy from the left lead is defined as  $\Sigma_L^{a,<}(t', t) = v g_L^{a,<}(t', t) v^+$ , where  $g_L(t', t) = g_L(t' - t)$  stands for the left lead's propagator, when decoupled from the system (this propagator depends only on the time difference since the decoupled lead is time independent in this gauge). We define the Fourier transform of  $g$  as

$$g(\omega) = \int_{-\infty}^{\infty} dt e^{i\omega t} g(t)$$

The retarded propagator in Fourier space is

$$g_L^r(\omega) = \frac{1}{\omega - h_L + i\eta}$$

while the advanced  $g_L^r(\omega) = [g_L^a(\omega)]^+$ . One can compute  $g_L^<(\omega) = i f(\omega) A_L(\omega)$ , where  $f(\omega) = 1/(e^{\omega/k_B T} + 1)$  is the Fermi distribution in the leads, and  $A_L(\omega) = i(g_L^r(\omega) - g_L^a(\omega))$  is the Nambu spectral function. The  $g_{L/R}^r$  [and in particular  $A_{L/R}(\omega)$ ] is assumed known, or at least easily obtainable from  $h_{L/R}$  and  $v$ . Finally, the Green functions  $G^r(t', t)$  and  $G^<(t', t)$  correspond to the propagator for the full system, including the coupling to the leads. (Note that, in practice, since  $G$  is inside a trace in  $J(t)$ , only matrix elements of  $G$  inside the  $S$  portion of the full system are needed). The retarded  $G^r$  satisfies the equation of motion

$$[i\partial_{t'} - H(t')] G(t', t) = \delta(t' - t)$$

while  $G^<$  (when projected onto the finite-dimensional system  $S$ ) satisfies the Keldysh relation

$$G^<(t', t) = \int dt_1 dt_2 G^r(t', t_1) \times [\Sigma_L^<(t_1 - t_2) + \Sigma_R^<(t_1 - t_2)] G^a(t_2, t)$$

Since  $h_S$  in  $H$  is time dependent,  $G$  propagators depend on two times; unlike  $\Sigma_{L/R}$  or  $g_{L/R}$  they are not Fourier diagonal. Instead, we can exploit the steady-state condition, which reads

$$G(t', t) = G(t' + \frac{2\pi}{\omega_0}, t + \frac{2\pi}{\omega_0})$$

to expand the system  $G$  as a Fourier transform in  $t' - t$  and a Fourier series in  $t$ . We define

$$G(t', t) = \sum_n e^{-in\omega_0 t} \int_{-\infty}^{\infty} \frac{d\epsilon}{2\pi} e^{-i\epsilon(t' - t)} G_n(\epsilon)$$

The natural question is how the equation of motion is expressed in terms of the harmonics  $G_n(\epsilon)$ . It takes the most convenient form if we redefine  $G_n(\epsilon)$  (where  $\epsilon$  is unbounded) in terms of the quasienergy  $\tilde{\epsilon} \in [0, \hbar\omega_0]$ , i.e.  $\epsilon = \tilde{\epsilon} + m\omega_0$

$$G_{mn}(\tilde{\epsilon}) = G_{m-n}(\tilde{\epsilon} + m\omega_0)$$

This has the advantage that the equation of motion translates to a matrix equation analogous to that of a static system in Fourier space

$$\sum_m (\tilde{\epsilon} + n'\omega_0 - H_{n'm}) G_{mn}^r(\tilde{\epsilon}) = \delta_{n'n}$$

where

$$H_{n'n} = \int dt e^{i(n'-n)t} H(t).$$

This is known as the Floquet description of the steady state dynamics in terms of sidebands, which appear formally as a new quantum number  $n$ . Time dependent portions of  $H(t)$  act as a coupling between different sidebands. The effective Hamiltonian for the  $n$ -th sideband is the static portion of  $H(t)$ , shifted by  $-n\omega_0$ . One therefore sometimes defines the Floquet “Hamiltonian” of the

system as

$$\mathbf{h}_{Snm} = h_{Snm} - n\omega_0 \delta_{nm}.$$

where, as before,  $h_{S'n'n} = \int dt e^{i(n'-n)t} h_S(t)$ . Likewise, one may define the retarded, lesser and advanced Floquet self-energies ( $\alpha = r, <, a$ ) as

$$\Sigma_{Lnm}^{\alpha}(\tilde{\epsilon}) = \delta_{nm} \Sigma_{L/R}^{\alpha}(\tilde{\epsilon} + n\omega_0)$$

(since the leads are static, the  $\Sigma_{L/R}^{\alpha}$  are sideband-diagonal).

The Floquet equation of motion for  $G_{nm}^r(\tilde{\epsilon})$  can be solved like in the case of a static system. Within the  $S$  portion of the system, we have

$$\mathbf{G}^r(\tilde{\epsilon}) = [\tilde{\epsilon} - \mathbf{h}_S - \Sigma_L^r(\tilde{\epsilon}) - \Sigma_R^r(\tilde{\epsilon})]^{-1}$$

Boldface denotes the sideband structure implicit in all the above matrices. Similarly, the Keldysh relation takes the simple form

$$\mathbf{G}^<(\tilde{\epsilon}) = \mathbf{G}^r(\tilde{\epsilon}) [\Sigma_L^<(\tilde{\epsilon}) + \Sigma_R^<(\tilde{\epsilon})] \mathbf{G}^a(\tilde{\epsilon})$$

Finally, the time averaged current  $I_{dc} \equiv I_0$  takes the form

$$I_{dc} = 2G_0 \int_0^{\hbar\omega} d\tilde{\epsilon} \text{ReTr} \{ [\mathbf{G}^r(\tilde{\epsilon}) \Sigma_L^<(\tilde{\epsilon}) + \mathbf{G}^<(\tilde{\epsilon}) \Sigma_L^a(\tilde{\epsilon})] \tau_z \}$$

where the trace includes the sideband index. In a practical computation, the number of sidebands that must be employed is finite, and depends on the applied voltage bias  $V$  (the typical number scales as  $n_{\text{max}} \sim v_0/V$ ). We employ an adaptive scheme that increases the number of sidebands recursively until convergence for each value of  $V$ .

---

[1] R. M. Lutchyn, J. D. Sau, and S. Das Sarma, Phys. Rev. Lett. **105**, 077001 (2010).  
[2] Y. Oreg, G. Refael, and F. von Oppen, Phys. Rev. Lett. **105**, 177002 (2010).  
[3] V. Mourik, K. Zuo, S. M. Frolov, S. R. Plissard, E. P. A. M. Bakkers, and L. P. Kouwenhoven, Science **336**, 1003 (2012).  
[4] M. T. Deng, C. L. Yu, G. Y. Huang, M. Larsson, P. Caroff, and H. Q. Xu, Nano Lett. **12**, 6414 (2012).  
[5] A. Das, Y. Ronen, Y. Most, Y. Oreg, M. Heiblum, and H. Shtrikman, Nat Phys **8**, 887 (2012).  
[6] K. Sengupta, I. Zutik, H.-J. Kwon, V. M. Yakovenko, and S. Das Sarma, Phys. Rev. B **63**, 144531 (2001).  
[7] C. J. Bolech and E. Demler, Phys. Rev. Lett. **98**, 237002 (2007).  
[8] K. T. Law, P. A. Lee, and T. K. Ng, Phys. Rev. Lett. **103**, 237001 (2009).  
[9] E. Prada, P. San-Jose, and R. Aguado, Phys. Rev. B **86**, 180503(R) (2012).  
[10] F. Pientka, G. Kells, A. Romito, P. W. Brouwer, and F. von Oppen, Phys. Rev. Lett. **109**, 227006 (2012).  
[11] D. Bagrets and A. Altland, Phys. Rev. Lett. **109**, 227005 (2012).  
[12] J. Liu, A. C. Potter, K. T. Law, and P. A. Lee, Phys. Rev. Lett. **109**, 267002 (2012).  
[13] E. J. H. Lee, X. Jiang, R. Aguado, G. Katsaros, C. M. Lieber, and S. De Franceschi, Phys. Rev. Lett. **109**, 186802 (2012).  
[14] C. Nayak, S. Simon, A. Stern, M. Freedman, and S. Das Sarma, Rev. Mod. Phys. **80**, 1083 (2008).  
[15] A. Y. Kitaev, Phys. Usp. **44**, 131 (2001).  
[16] H. Kwon, K. Sengupta, and V. Yakovenko, Eur. Phys. J. B **37**, 349 (2003).  
[17] L. Fu and C. L. Kane, Phys. Rev. B **79**, 161408 (2009).  
[18] D. M. Badiane, M. Houzet, and J. S. Meyer, Phys. Rev. Lett. **107**, 177002 (2011).  
[19] P. San-Jose, E. Prada, and R. Aguado, Phys. Rev. Lett. **108**, 257001 (2012).  
[20] D. I. Pikulin and Y. V. Nazarov, Phys. Rev. B **86**, 140504 (2012).  
[21] Shapiro step experiments [16] are in principle another route to unveil the anomalous effect. Indeed, the first

encouraging experiments along these lines have been recently reported, see L. P. Rokhinson, X. Liu, and J. K. Furdyna, *Nature Physics* **8**, 795 (2012).

[22] Y.-J. Doh, J. A. van Dam, A. L. Roest, E. P. A. M. Bakkers, L. P. Kouwenhoven, and S. De Franceschi, *Science* **309**, 272 (2005).

[23] H. A. Nilsson, P. Samuelsson, P. Caroff, and H. Q. Xu, *Nano Lett.* **12**, 228 (2012).

[24] J. Alicea, *Rep. Prog. Phys.* **75**, 076501 (2012).

[25] Note that  $\Delta_-$  is at momentum  $p = 0$  only for  $B > B_h$ , where  $B_h \equiv \mu < B_c$ . Otherwise, it is at a finite but small momentum. However, as  $B$  approaches  $B_c$ ,  $\Delta_-$  is centered at  $p = 0$  and is approximately equal to  $|E_0|$ , where  $E_0$  is the zero momentum energy of the lowest subband,  $E_0 = B - B_c$ , and is related to the topological charge of the lowest superconducting band. [39].

[26] C. Beenakker, in *Transport phenomena in mesoscopic systems: proceedings of the 14th Taniguchi symposium, Shima, Japan, November 10-14, 1991* (Springer-Verlag, 1992) p. 235.

[27] D. Averin and A. Bardas, *Phys. Rev. Lett.* **75**, 1831 (1995).

[28] J. C. Cuevas, A. Martín-Rodero, and A. L. Yeyati, *Phys. Rev. B* **54**, 7366 (1996).

[29] Q.-f. Sun, H. Guo, and J. Wang, *Phys. Rev. B* **65**, 075315 (2002).

[30] Note that the small step visible at  $eV = \Delta_{\text{eff}}/2$  is the second MAR harmonic, whose relative height vanishes as  $T_N \rightarrow 0$ .

[31] Similar considerations may apply to recent experiments with lead nanoconstrictions formed in an STM tip, see J. G. Rodrigo et al, *Phys. Rev. Lett.*, **109**, 237003 (2012).

[32] G. Johansson, E. N. Bratus, V. S. Shumeiko, and G. Wendum, *Phys. Rev. B* **60**, 1382 (1999).

[33] A. L. Yeyati, A. Martín-Rodero, and E. Vecino, *Phys. Rev. Lett.* **91**, 266802 (2003).

[34] T. Jonckheere, A. Zazunov, K. V. Bayandin, V. Shumeiko, and T. Martin, *Phys. Rev. B* **80**, 184510 (2009).

[35] J. C. Cuevas and M. Fogelström, *Phys. Rev. B* **64**, 104502 (2001).

[36] Note that residual splitting may survive in the topological phase for finite length nanowires, for which a finite (albeit exponentially small) coupling between four MBSs exist.

[37] M. Chauvin, P. vom Stein, D. Esteve, C. Urbina, J. C. Cuevas, and A. L. Yeyati, *Phys. Rev. Lett.* **99**, 067008 (2007).

[38] H. Haug and A. Jauho, *Quantum kinetics in transport and optics of semiconductors*, Vol. 123 (Springer, 2007).

[39] P. Ghosh, J. D. Sau, S. Tewari, and S. Das Sarma, *Phys. Rev. B* **82**, 184525 (2010).